Investigating the role of neutral particles in the linear device Magnum-PSI

Ivo Classen, Hennie van der Meiden, Gijs Akkermans, Renato Perillo, Jonathan van den Berg, Richard Engeln

DIFFER

NWO

Outlook

- Introduction to Magnum-PSI

- A: Detachment studies in Magnum-PSI
- B: Investigating Nitrogen chemistry: N-MAR
- C: Plasma-neutral interaction in the pre-sheath

- D: Plans for VUV-LIF on Magnum-PSI: $H_2(r,\nu)$

Magnum-PSI

- Cascaded arc plasma source:
  H, D, He, Ar, …
- Superconducting magnet
- Target manipulator + TEAC
- Many diagnostics
  - TS, CTS
  - OES, fast camera, bolometer
  - IR, pyrometer, Probes, calorimetry
  - ….

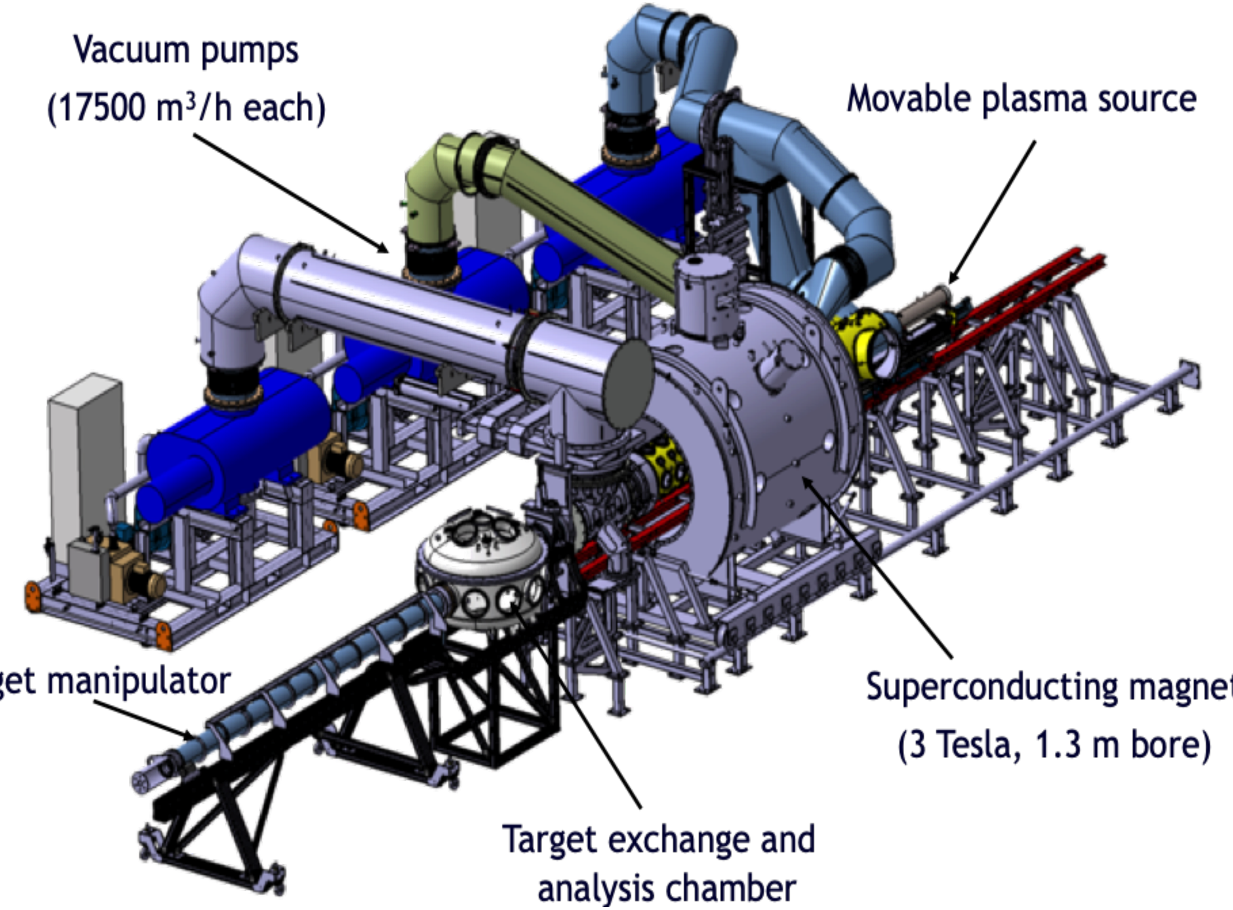

Magnum-PSI as a divertor simulator

T_e up to 5 eV

$n_e = 10^{19} - 10^{21}$ m^{-3}

Γ_i up to 10^{25} m^{-2}s^{-1}

q up to 50 MWm^{-2}

Pulses: up to 20eV and 1GWm^{-2}

Differential pumping:

neutrals: 0.3 Pa during plasma

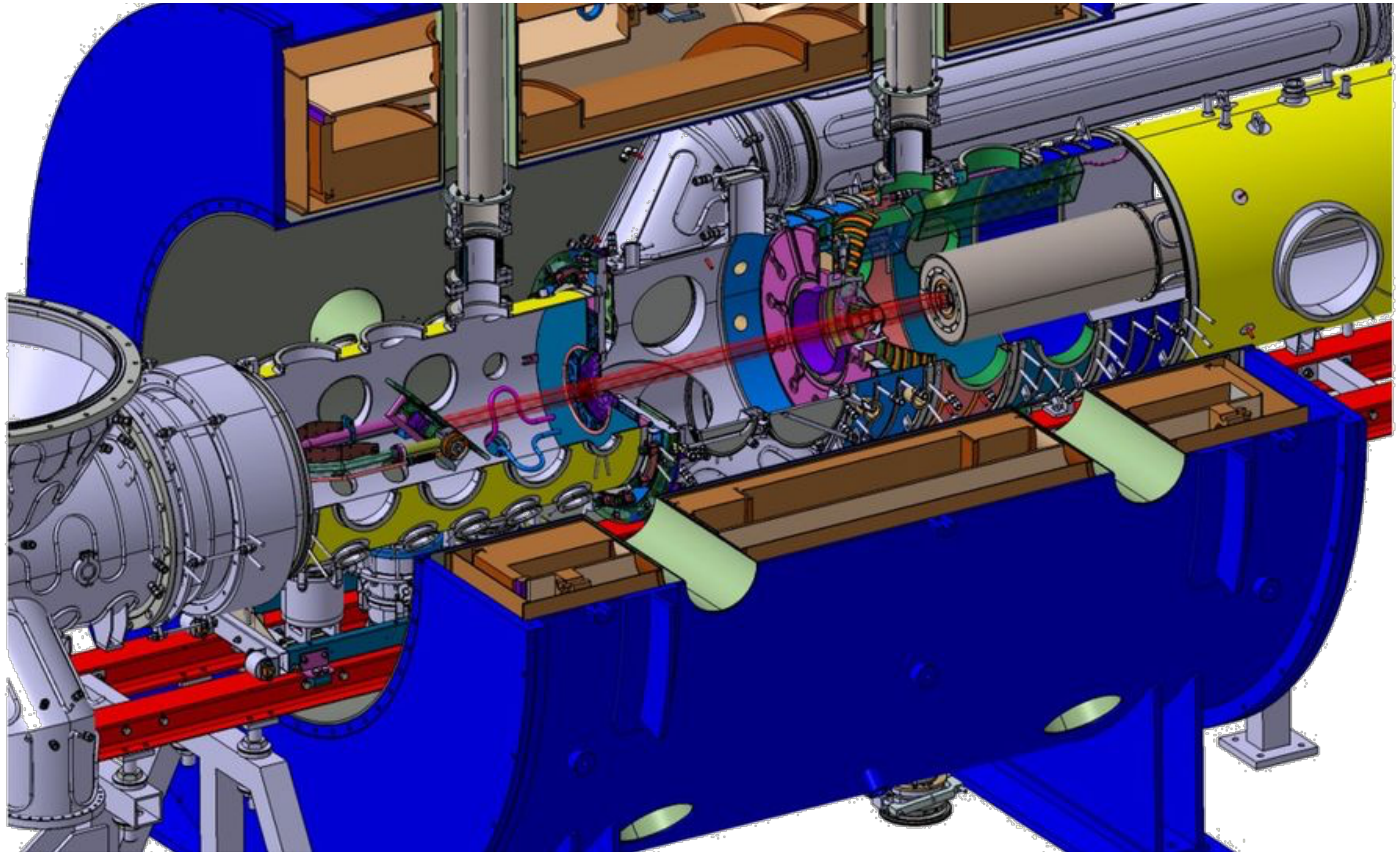

Section A
Detachment studies in Magnum-PSI

Gijs Akkermans et al.

PoP, **27** (2020) 102509

Simulating detachment in Magnum

Seeding gas in target chamber simulates detached states

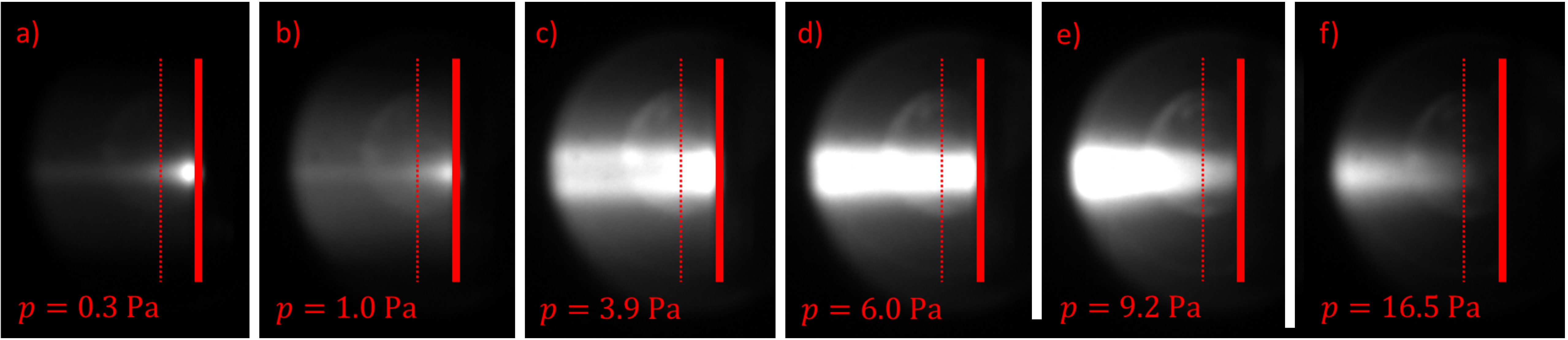

Higher neutral background pressure →

Pressure and Fluxes strongly reduced

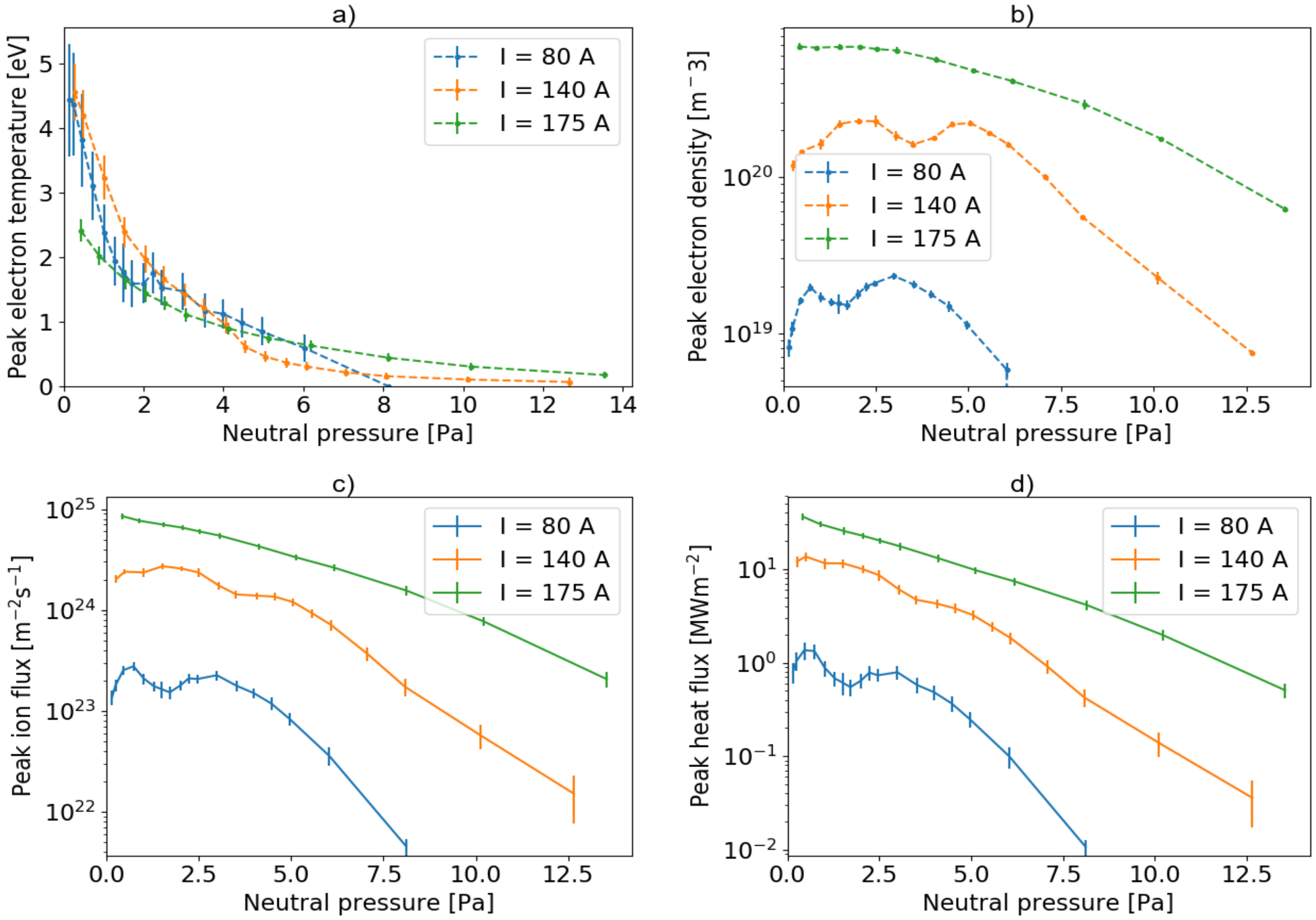

Balmer: 3 regimes

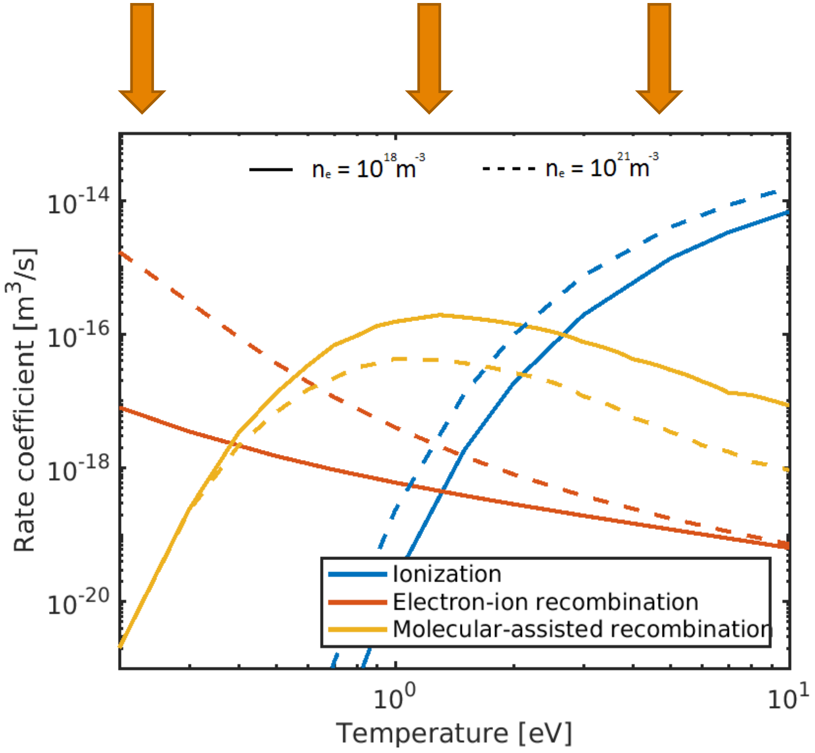

0.3 Pa
$T_e =$ 4.5 eV
Peaked
Overpopulated

3.5 Pa
$T_e =$ 1.2 eV
Hollow

12.7 Pa
$T_e =$ 0.06 eV
Peaked
Underpopulated

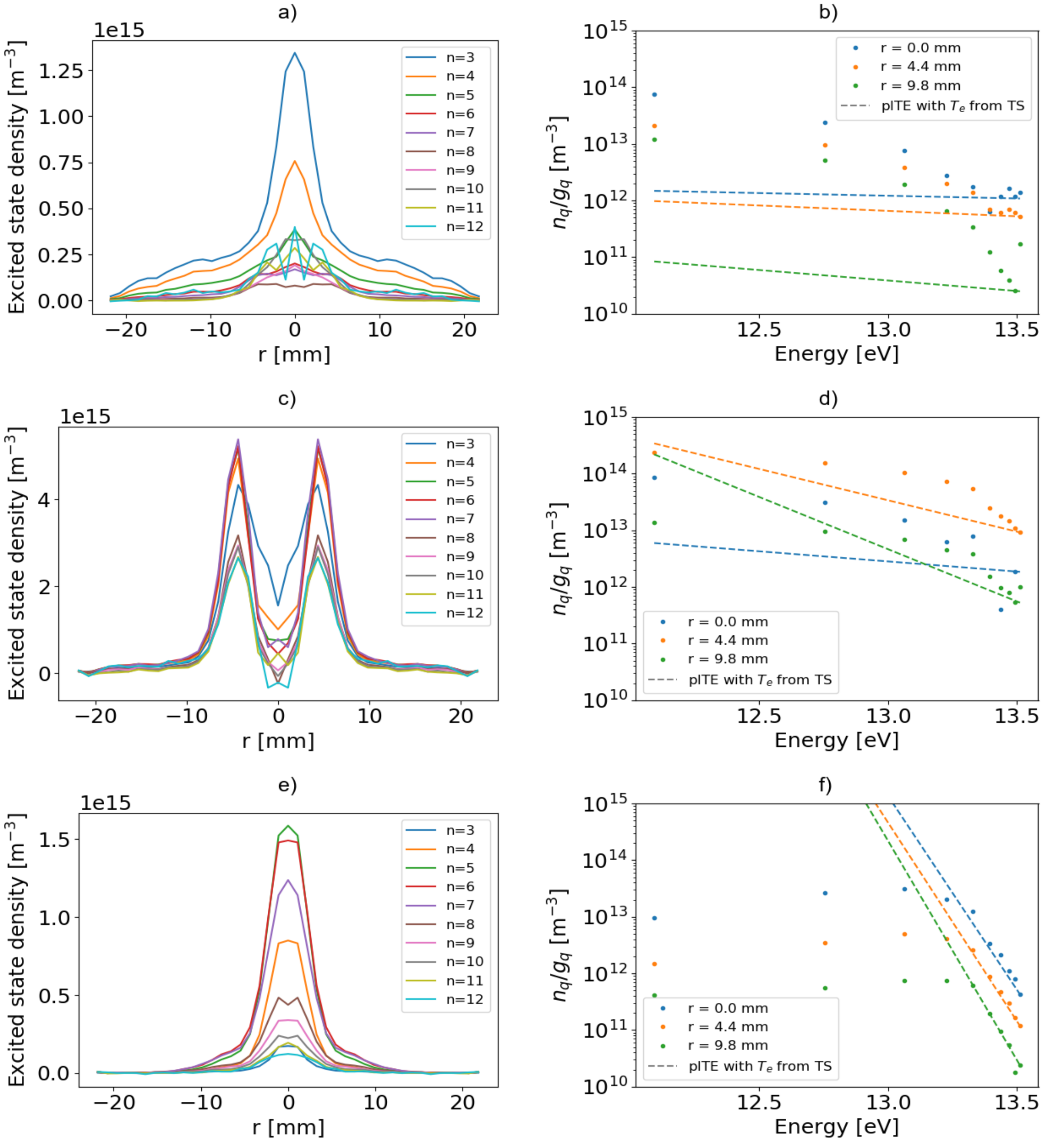

Fulcher Band measurements

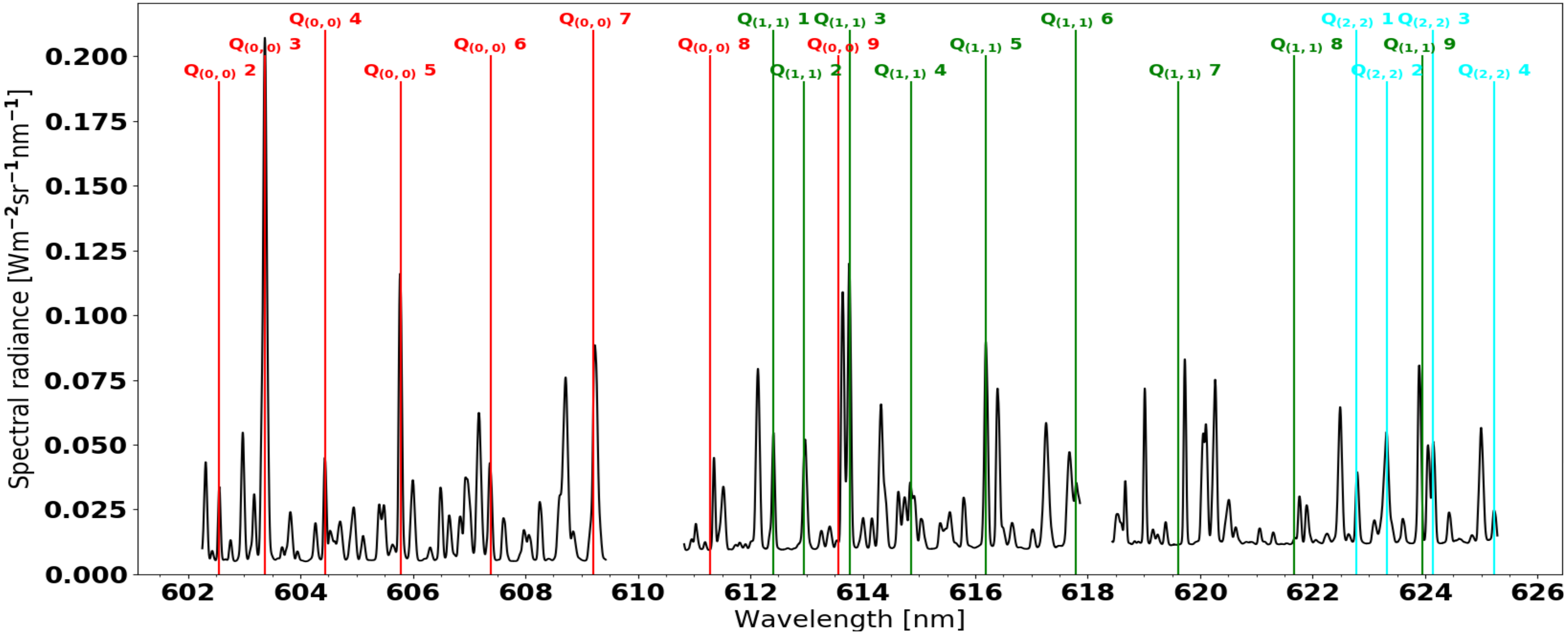

$Q_{(0,0)}$, $Q_{(1,1)}$ and $Q_{(2,2)}$ branches

No hollow profiles observed

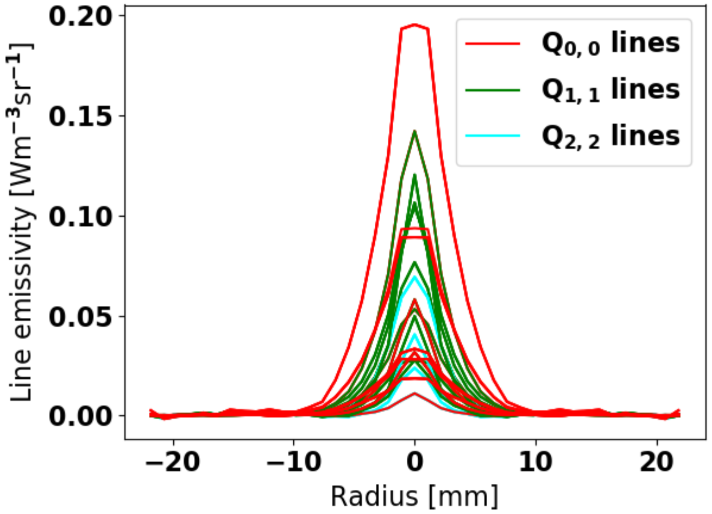

Fitting rotational and vibrational temperatures

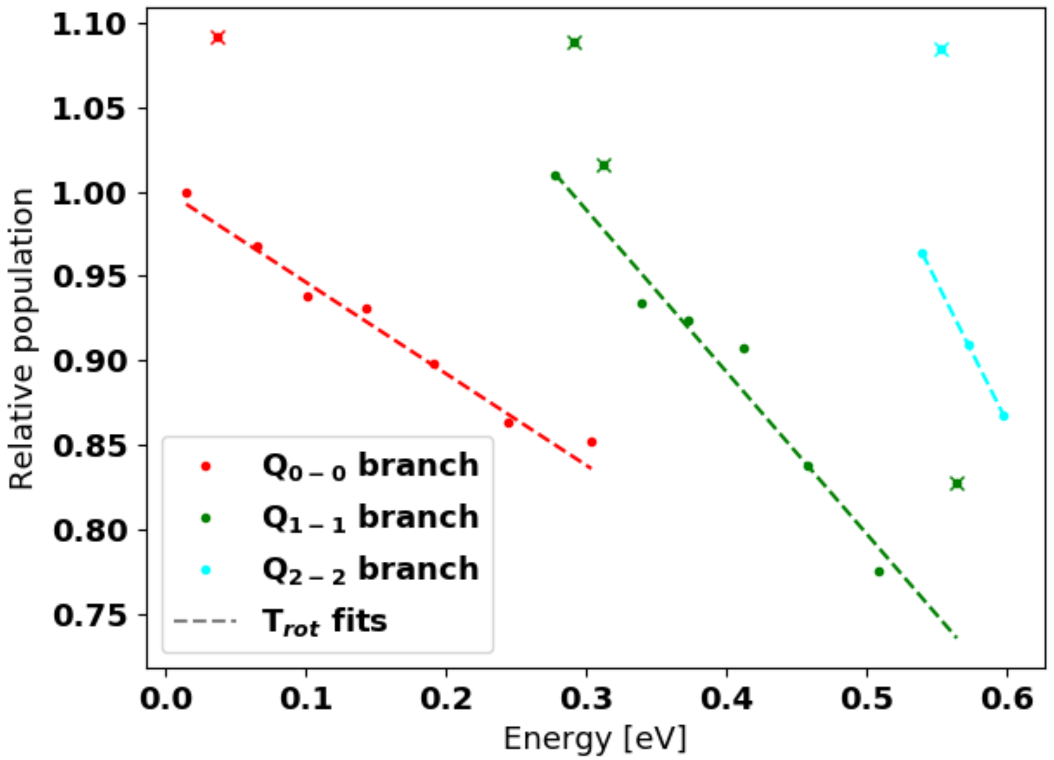

Higher branches have lower T_{rot}

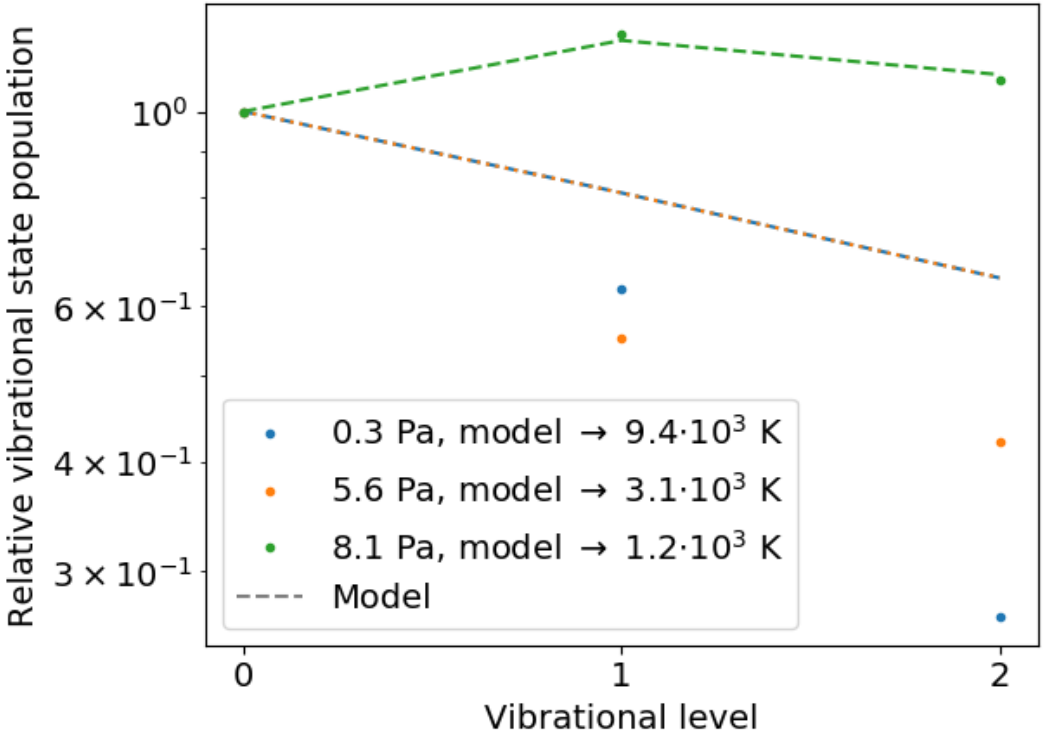

Fitting for T_{vib} fails at low neutral densities

(Franck-Condon excitation from ground state in Boltzmann distribution)

Detachment scan: Temperatures and reaction rates

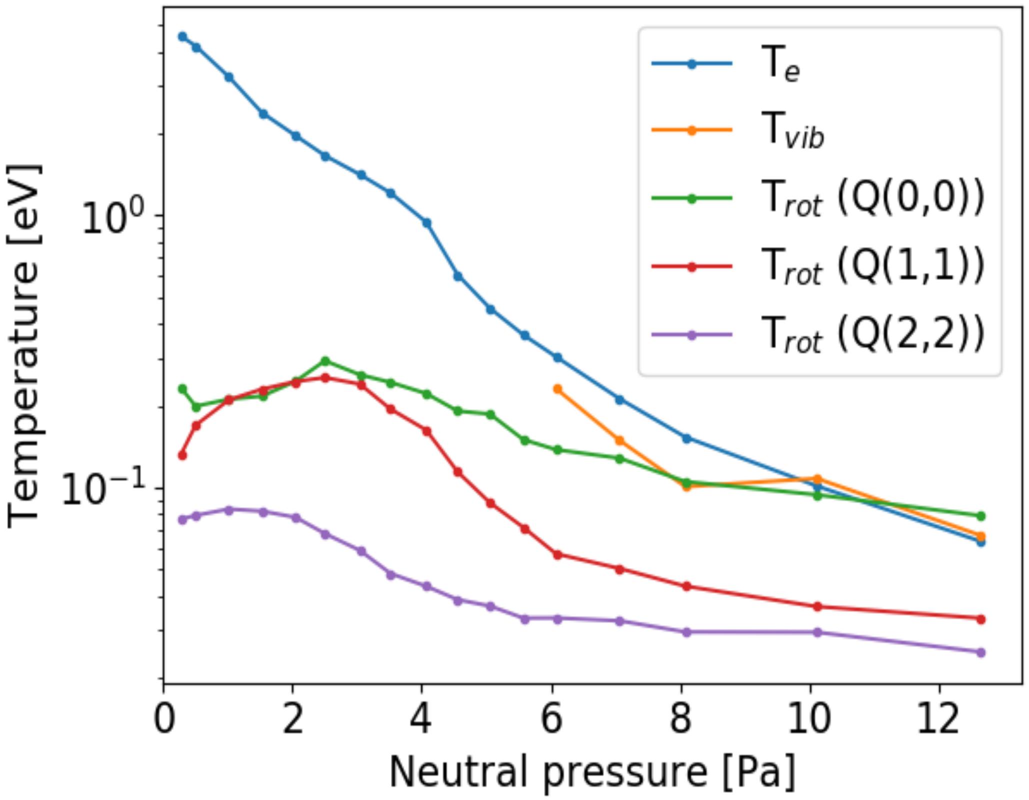

Ionization, MAR, recombination

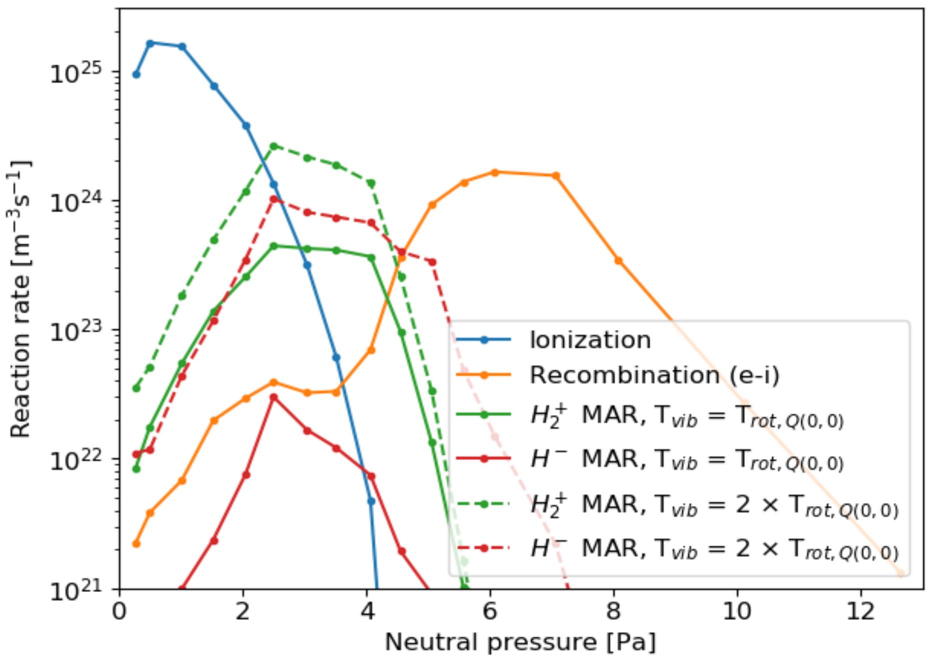

➔ Better measurement of T_{vib} needed

Section B
Investigating Nitrogen chemistry: N-MAR

Renato Perillo et al.

PoP, **26** (2019) 102502

PPCF, **60** (2018) 105004

Global model of H_2 + N_2 plasma chemistry

H_2 species	N_2 species	H_2-N_2 species
$H, H_2, H^+, H_2^+, H_2(v_{n=4}), H_3^+$	$N_2, N, N_2^*(A^3\Sigma), N_2^+, N^+$	$NH, NH_2, NH_3, NH_3^+, NH_2^+, NH^+, N_2H^+, NH_4^+$

N#.	Reaction	Rate coefficient (cm³s⁻¹)	Reference
1	$H + e^- \rightarrow H^+ + 2e^-$	from cross section	[96]
2	$H_2 + e^- \rightarrow H_2^+ + 2e^-$	from cross section	[96]
3	$N + e^- \rightarrow N^+ + 2e^-$	from cross section	[97]
4	$N_2 + e^- \rightarrow N_2^+ + 2e^-$	from cross section	[97]
5	$N_2 + e^- \rightarrow N_2^*(A^3\Sigma) + e^-$	from cross section	[98]
6	$N_2^*(A^3\Sigma) + e^- \rightarrow N_2^+ + 2e^-$	from cross section	[57]
7	$N_2 + e^- \rightarrow N^+ + N + 2e^-$	$2.9 \times 10^{-9} \times T_e^{0.72} \times exp(-29.71/T_e)$	[99]
8	$H_2 + e^- \rightarrow H^+ + H + 2e^-$	$9.4 \times 10^{-10} \times T_e^{0.45} \times exp(-29.94/T_e)$	[100]
9	$H_2 + e^- \rightarrow H_2v_{n=4} + e^-$	$6.7 \times 10^{-10} \times T_e^{1.82} \times exp(-1.89/T_e)$	[66]
10	$NH + e^- \rightarrow NH^+ + 2e^-$	$2.1 \times 10^{-8} \times T_e^{0.37} \times exp(-15.49/T_e)$	[101]
11	$NH + e^- \rightarrow N^+ + H + 2e^-$	$7.6 \times 10^{-9} \times T_e^{0.29} \times exp(-16.82/T_e)$	[101]
12	$NH_2 + e^- \rightarrow NH_2^+ + 2e^-$	$1.3 \times 10^{-8} \times T_e^{0.5} \times exp(-12.4/T_e)$	[101]
13	$NH_2 + e^- \rightarrow NH^+ + H + 2e^-$	$2.2 \times 10^{-8} \times T_e^{0.21} \times exp(-17.97/T_e)$	[101]
14	$NH_3 + e^- \rightarrow NH_3^+ + 2e^-$	$1.5 \times 10^{-8} \times T_e^{0.4} \times exp(-13.61/T_e)$	[101]
15	$NH_3 + e^- \rightarrow NH_2^+ + H + 2e^-$	$1.6 \times 10^{-8} * T_e^{0.34} \times exp(-15.41/T_e)$	[101]
16	$NH_3 + e^- \rightarrow NH^+ + H + H + 2e^-$	$5.4 \times 10^{-10} \times T_e^{0.37} \times exp(-26.06/T_e)$	[101]
17	$NH_3 + e^- \rightarrow N^+ + H + H_2 + 2e^-$	$8.8 \times 10^{-11} \times T_e^{0.59} \times exp(-29/T_e)$	[102]
18	$NH_3 + e^- \rightarrow H^+ + NH_2 + 2e^-$	$1.3 \times 10^{-10} \times T_e^{0.47} \times exp(-28.55/T_e)$	[102]
19	$H_2^+ + e^- \rightarrow H + H$	$1.6 \times 10^{-8} \times (T_e/0.026)^{-0.43}$	[103]
20	$H_3^+ + e^- \rightarrow H_2 + H$	$2.34 \times 10^{-8} \times (T_e/0.026)^{-0.52}$	[104]
21	$H_3^+ + e^- \rightarrow H + H + H$	$4.36 \times 10^{-8} \times (T_e/0.026)^{-0.52}$	[104]
22	$N_2^+ + e^- \rightarrow N + N$	$1.7 \times 10^{-7} \times (T_e/0.026)^{-0.3}$	[105]
23	$NH^+ + e^- \rightarrow N + H$	$4.3 \times 10^{-8} \times (T_e/0.026)^{-0.5}$	[103]
24	$NH_2^+ + e^- \rightarrow NH + H$	$1.02 \times 10^{-7} \times (T_e/0.026)^{-0.4}$	[106]
25	$NH_2^+ + e^- \rightarrow N + H_2$	$1.98 \times 10^{-8} \times (T_e/0.026)^{-0.4}$	[106]
26	$NH_3^+ + e^- \rightarrow NH + 2H$	$1.55 \times 10^{-7} \times (T_e/0.026)^{-0.5}$	[103]
27	$NH_3^+ + e^- \rightarrow NH_2 + H$	$1.55 \times 10^{-7} \times (T_e/0.026)^{-0.5}$	[103]
28	$NH_4^+ + e^- \rightarrow NH_3 + H$	$8.49 \times 10^{-7} \times (T_e/0.026)^{-0.6}$	[106]
29	$NH_4^+ + e^- \rightarrow NH_2 + 2H$	$3.77 \times 10^{-8} \times (T_e/0.026)^{-0.6}$	[106]
30	$N_2H^+ + e^- \rightarrow N_2 + H$	$5.13 \times 10^{-8} \times (T_e/0.026)^{-0.72}$	[107]
31	$N_2H^+ + e^- \rightarrow NH + N$	$2.09 \times 10^{-8} \times (T_e/0.026)^{-0.72}$	[108]
32	$N_2 + e^- \rightarrow N + N + e^-$	$2.4 \times 10^{-8} \times T_e^{0.27} \times exp(-15.53/T_e)$	[99]
33	$H_2 + e^- \rightarrow H + H + e^-$	$8.4 \times 10^{-8} \times T_e^{-0.45} \times exp(-11.18/T_e)$	[100]
34	$NH + e^- \rightarrow N + H + e^-$	$4.7 \times 10^{-8} \times T_e^{-0.22} \times exp(-7.69/T_e)$	[109]
35	$NH_2 + e^- \rightarrow NH + H + e^-$	$4.5 \times 10^{-8} \times T_e^{-0.22} \times exp(-7.61/T_e)$	[109]
36	$NH_2 + e^- \rightarrow N + H_2 + e^-$	$1.5 \times 10^{-8} \times T_e^{0.38} \times exp(-11.44/T_e)$	[109]
37	$NH_3 + e^- \rightarrow NH + H + H + e^-$	$1.3 \times 10^{-8} \times T_e^{0.38} \times exp(-11.06/T_e)$	[110]
38	$NH_3 + e^- \rightarrow NH_2 + H + e^-$	$4.2 \times 10^{-8} \times T_e^{-0.19} \times exp(-7.59/T_e)$	[110]
39	$NH_3 + e^- \rightarrow NH + H_2 + e^-$	$4.1 \times 10^{-8} \times T_e^{-0.26} \times exp(-4.81/T_e)$	[110]
40	$H_2 + NH \rightarrow NH_2 + H$	$5.96 \times 10^{-11} \times exp(-0.67/T_g)$	[111]
41	$NH_3 + H \rightarrow NH_2 + H_2$	$8.4 \times 10^{-14} \times (T_g/0.026)^{4.1} \times exp(-0.41/T_g)$	[112]
42	$NH + NH_2 \rightarrow NH_3 + N$	1.66×10^{-12}	[112]
43	$N + NH_2 \rightarrow N_2 + H_2$	1.2×10^{-10}	[113]
44	$NH_2 + H_2 \rightarrow NH_3 + H$	$5.4 \times 10^{-11} \times exp(-0.56/T_g)$	[114]
45	$NH + NH \rightarrow NH_2 + N$	$1.7 \times 10^{-12} \times (T_g/0.026)^{1.5}$	[115]
46	$NH + NH \rightarrow N_2 + H + H$	8.5×10^{-11}	[56]
47	$NH_2 + H \rightarrow NH + H_2$	$6.6 \times 10^{-11} \times exp(-0.1586/T_g)$	[116]
48	$NH + NH \rightarrow N_2 + H_2$	$5 \times 10^{-14} \times (T_g/0.026)$	[116]
49	$H_2 + N \rightarrow NH + H$	$4.65 \times 10^{-11} \times exp(-1.43/T_g)$	[111]
50	$N + NH \rightarrow N_2 + H$	5×10^{-11}	[113]
51	$NH + H \rightarrow N + H_2$	$5.4 \times 10^{-11} \times exp(-0.0142/T_g)$	[116]
52	$N^+ + H_2 \rightarrow NH^+ + H$	5×10^{-10}	[117]
53	$N^+ + NH_2 \rightarrow NH_2^+ + N$	1×10^{-9}	[118]
54	$N^+ + H \rightarrow H^+ + N$	2×10^{-10}	[119]
55	$N^+ + N_2 \rightarrow N + N_2^+$	2×10^{-11}	[117]
56	$N^+ + NH \rightarrow NH^+ + N$	$3.7 \times 10^{-10} \times (T_g/0.026)^{-0.5}$	[118]
57	$N^+ + NH_3 \rightarrow N_2H^+ + H_2$	2.1×10^{-10}	[117]
58	$N^+ + NH \rightarrow N_2^+ + H$	$3.7 \times 10^{-10} \times (T_g/0.026)^{-0.5}$	[118]
59	$N^+ + NH_3 \rightarrow NH_3^+ + N$	1.7×10^{-9}	[117]
60	$N^+ + NH_3 \rightarrow NH_2^+ + NH$	4.7×10^{-10}	[117]
61	$H^+ + NH_3 \rightarrow NH_3^+ + H$	$3.7 \times 10^{-9} \times (T_g/0.026)^{-0.5}$	[120]
62	$H^+ + NH \rightarrow NH^+ + H$	$2.1 \times 10^{-9} \times (T_g/0.026)^{-0.5}$	[118]
63	$H^+ + NH_2 \rightarrow NH_2^+ + H$	$2.9 \times 10^{-9} \times (T_g/0.026)^{-0.5}$	[118]
64	$H^+ + H_2v_{n=4} \rightarrow H + H_2^+$	2.5×10^{-9}	[36]
65	$H_2^+ + NH_3 \rightarrow H_2 + NH_3^+$	5.7×10^{-9}	[117]
66	$H_2^+ + N_2 \rightarrow N_2H^+ + H$	2×10^{-9}	[117]
67	$H_2^+ + N \rightarrow NH^+ + H$	1.9×10^{-9}	[118]
68	$H_2^+ + N \rightarrow N^+ + H_2$	5×10^{-10}	[118]
69	$H_2^+ + NH \rightarrow NH^+ + H_2$	$7.6 \times 10^{-10} \times (T_g/0.026)^{-0.5}$	[117]
70	$H_2^+ + NH_2 \rightarrow NH_2^+ + H_2$	$7.6 \times 10^{-10} \times (T_g/0.026)^{-0.5}$	[118]
71	$H_2^+ + NH \rightarrow NH_2^+ + H$	$2.1 \times 10^{-9} \times (T_g/0.026)^{-0.5}$	[118]
72	$H_2^+ + NH_2 \rightarrow NH_3^+ + H$	5×10^{-11}	[119]
73	$H_2^+ + NH_3 \rightarrow NH_4^+ + H$	5×10^{-11}	[119]
74	$H_2^+ + H_2 \rightarrow H_3^+ + H$	2×10^{-9}	[15]
75	$H_3^+ + N \rightarrow NH^+ + H_2$	2.6×10^{-10}	[15]
76	$H_3^+ + N \rightarrow NH_2^+ + H$	3.9×10^{-10}	[15]
77	$H_3^+ + NH_3 \rightarrow NH_4^+ + H_2$	$4.4 \times 10^{-9} \times (T_g/0.026)^{-0.5}$	[15]
78	$H_3^+ + NH_2 \rightarrow NH_3^+ + H_2$	$1.8 \times 10^{-9} \times (T_g/0.026)^{-0.5}$	[118]
79	$H_3^+ + NH \rightarrow NH_2^+ + H_2$	$1.3 \times 10^{-9} \times (T_g/0.026)^{-0.5}$	[118]
80	$H_3^+ + N_2 \rightarrow N_2H^+ + H_2$	1.9×10^{-9}	[15]
81	$N_2^*(A^3\Sigma) + H \rightarrow NH + N$	2.8×10^{-10}	[95]
82	$NH^+ + H_2 \rightarrow NH_2^+ + H$	1×10^{-9}	[95]
83	$NH^+ + N \rightarrow N_2^+ + H$	1.3×10^{-9}	[118]
84	$NH^+ + N_2 \rightarrow N_2H^+ + N$	6.5×10^{-10}	[117]
85	$NH^+ + NH \rightarrow NH_2^+ + N$	1×10^{-9}	[118]
86	$NH^+ + NH_2 \rightarrow NH_3^+ + N$	1.5×10^{-9}	[118]
87	$NH^+ + NH_2 \rightarrow NH_2^+ + NH$	1.8×10^{-9}	[119]
88	$NH^+ + NH_3 \rightarrow NH + NH_3^+$	1.8×10^{-9}	[119]
89	$NH^+ + NH_3 \rightarrow NH_4^+ + N$	6×10^{-10}	[117]
90	$NH_2^+ + N \rightarrow N_2H^+ + N$	9.1×10^{-11}	[118]
91	$NH_2^+ + NH \rightarrow NH_3^+ + N$	7.3×10^{-10}	[118]
92	$NH_2^+ + NH_3 \rightarrow NH_4^+ + NH$	1.2×10^{-9}	[117]
93	$NH_2^+ + NH_3 \rightarrow NH_2 + NH_3^+$	1.2×10^{-9}	[117]
94	$NH_2^+ + H_2 \rightarrow NH_3^+ + H$	2×10^{-10}	[117]
95	$NH_3^+ + NH_3 \rightarrow NH_4^+ + NH_2$	2.1×10^{-9}	[117]
96	$NH_3^+ + NH \rightarrow NH_4^+ + N$	$7.1 \times 10^{-10} \times (T_g/0.026)^{-0.5}$	[118]
97	$NH_3^+ + H_2 \rightarrow NH_4^+ + H$	4.4×10^{-13}	[117]
98	$N_2H^+ + NH_3 \rightarrow NH_4^+ + N_2$	2.3×10^{-9}	[117]
99	$N_2^+ + H_2 \rightarrow NH_2^+ + H$	2×10^{-9}	[117]
100	$N_2^+ + NH_3 \rightarrow N_2 + NH_3^+$	2×10^{-9}	[117]
101	$N_2^+ + N \rightarrow N_2 + N^+$	1×10^{-11}	[117]
102	$H_2 + e^- \rightarrow H_2 + e^-$	from cross section	[122]
103	$H + e^- \rightarrow H + e^-$	from cross section	[96]
104	$N_2 + e^- \rightarrow N_2 + e^-$	from cross section	[99]
105	$N + e^- \rightarrow N + e^-$	from cross section	[97]
106	$NH_3 + e^- \rightarrow NH_3 + e^-$	from cross section	[57]

Reduced set of reactions

Reaction	Type
$H + e^- \rightarrow H^+ + 2e^-$	*Ionization*
$H_2 + e^- \rightarrow H_2^+ + 2e^-$	*Ionization*
$N_2 + e^- \rightarrow N + N + e^-$	*Dissociation*
$H_2 + e^- \rightarrow H_2v + e^-$	*Vibrational excitation*
$H_2v + H^+ \rightarrow H_2^+ + H$	*Ion conversion*
$H_2^+ + e^- \rightarrow H + H$	*Dissociative recombination*
$H_2 + N \rightarrow NH + H$	*Atom transfer*
$N_2 + H_2^+ \rightarrow N_2H^+ + H$	*Proton transfer*
$N_2H^+ + e^- \rightarrow N_2 + H$	*Dissociative recombination*
$N_2H^+ + e^- \rightarrow NH + N$	*Dissociative recombination*
$NH + H^+ \rightarrow NH^+ + H$	*Ion conversion*
$NH^+ + e^- \rightarrow N + H$	*Dissociative recombination*
$H + e^- \rightarrow H + e^-$	*Elastic*
$H_2 + e^- \rightarrow H_2 + e^-$	*Elastic*
$N + e^- \rightarrow N + e^-$	*Elastic*
$N_2 + e^- \rightarrow N_2 + e^-$	*Elastic*

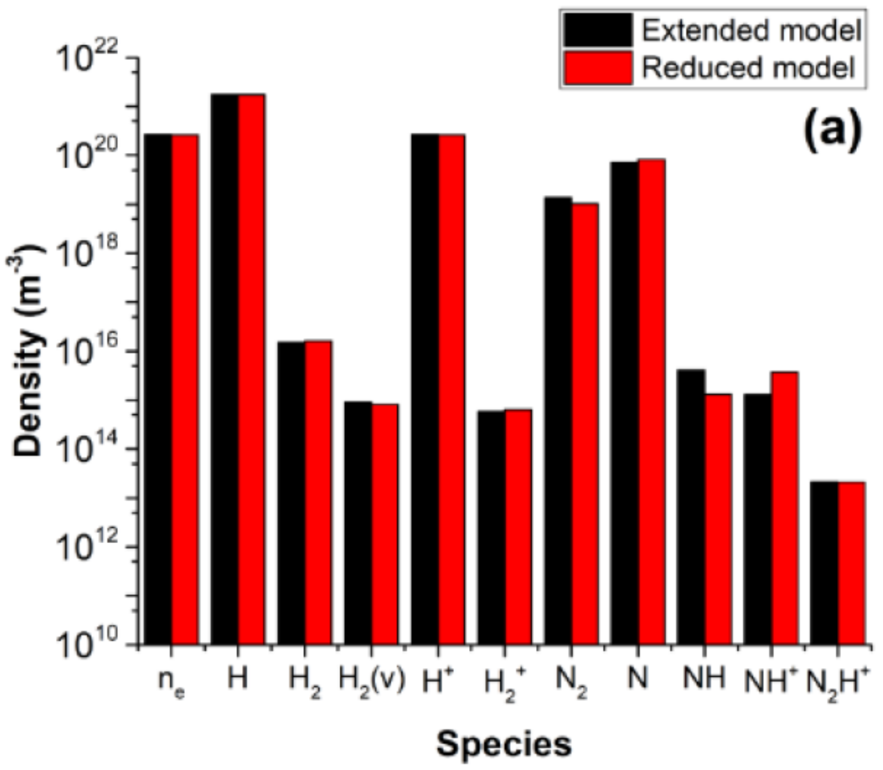

New recombination pathway: N-MAR

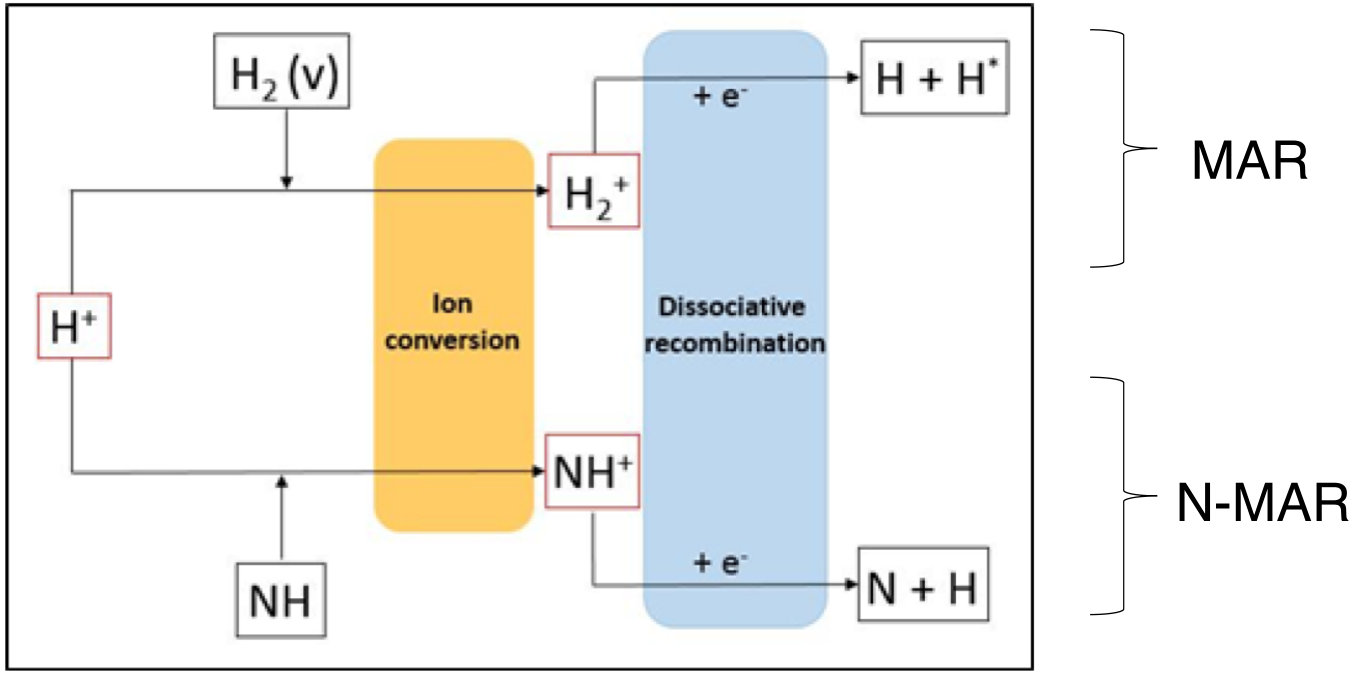

1) $H^+ + NH_x \rightarrow NH_x^+ + H$ *Ion conversion*

2) $NH_x^+ + e^- \rightarrow NH_{x-1} + H$ *Dissociative recombination*

Experimental evidence of N-MAR effect

Strong presence of NH observed

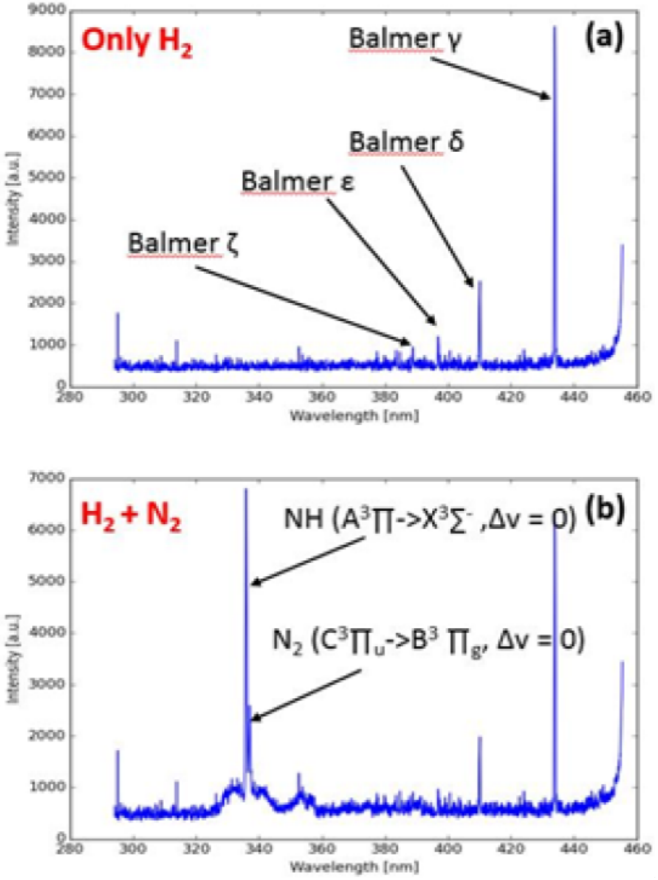

Pressure drops with N_2 content

@ constant P_{back} = 2Pa

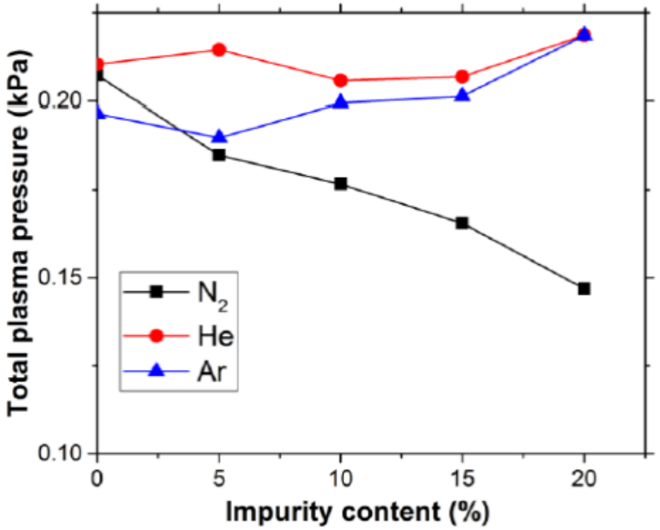

Density reduced: recombination

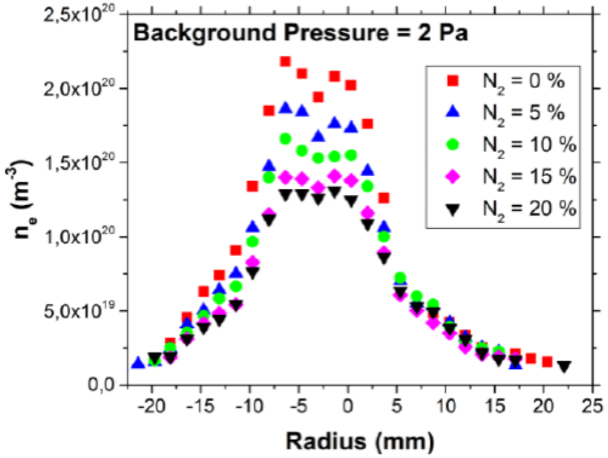

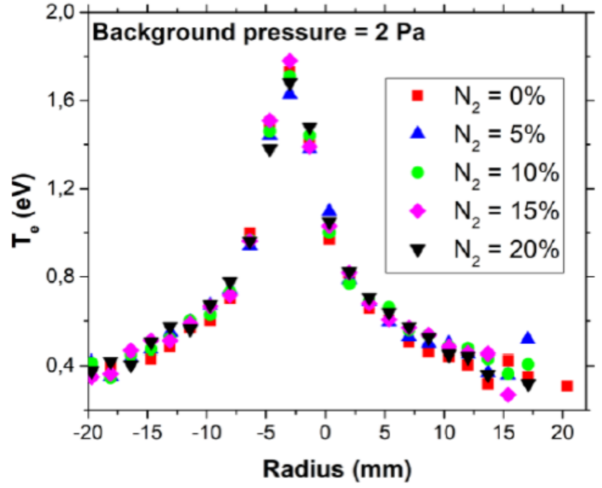

Nitrogen chemistry implemented in B2.5 Eunomia

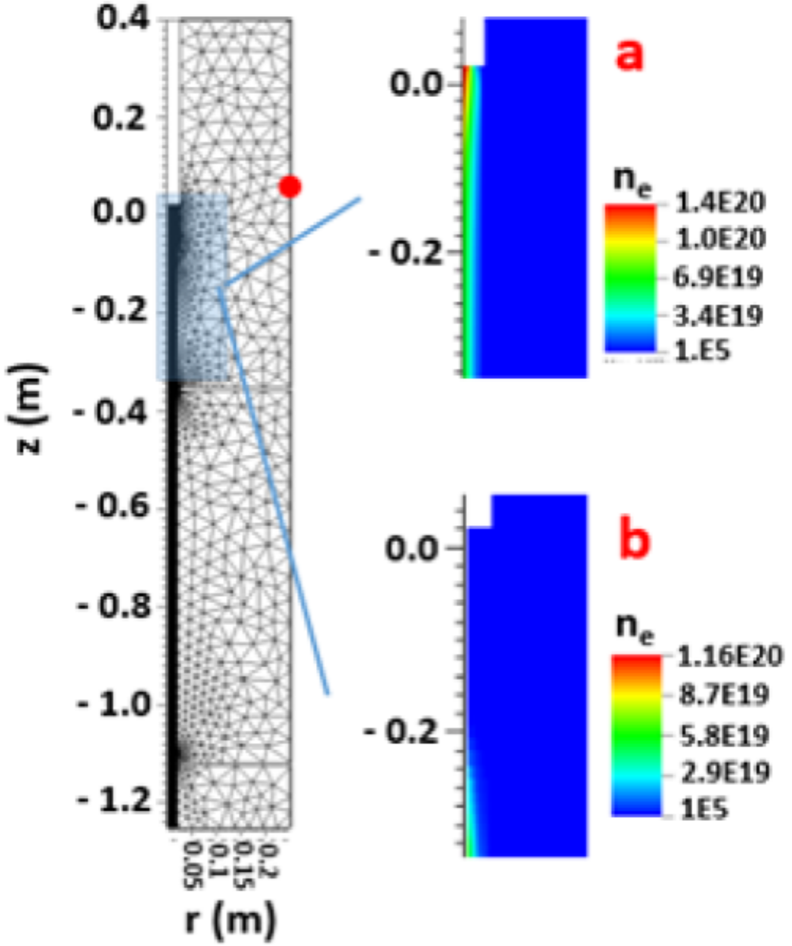

Reduction of plasma pressure reproduced

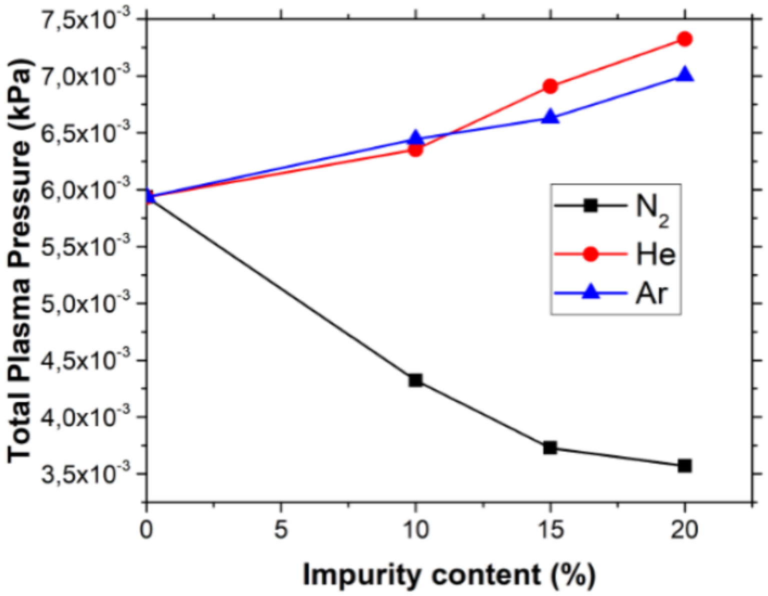

Importance of N-MAR

H density rises with N_2: recombination

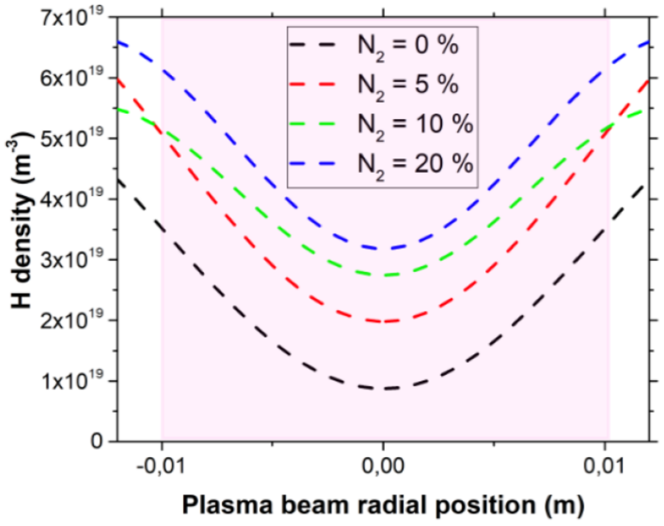

N-MAR most dominant N_2 process

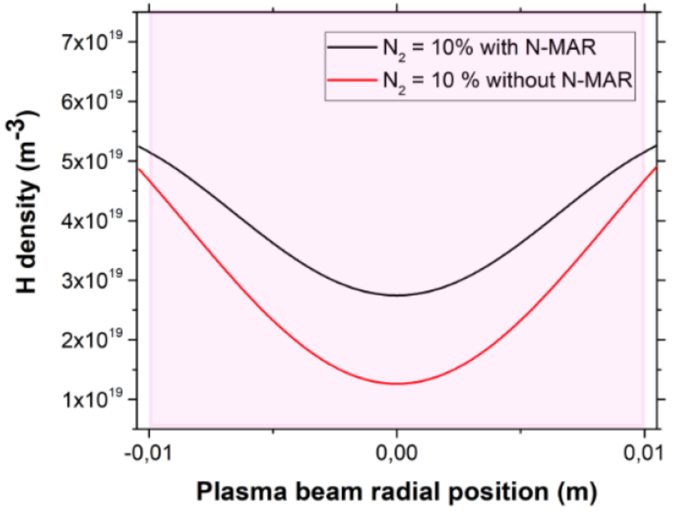

N-MAR dominates over MAR

N-MAR

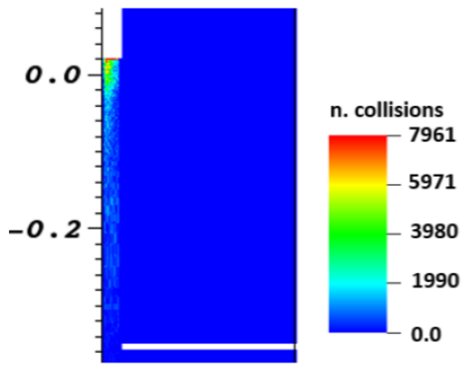

MAR

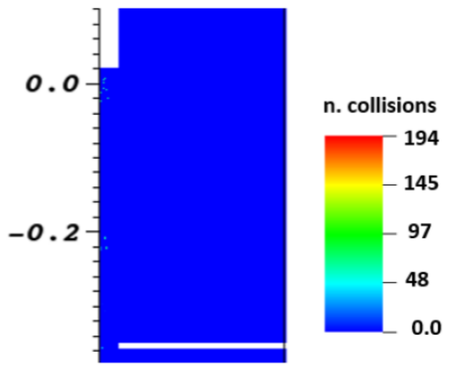

Section C
Plasma-neutral interaction in the pre-sheath

Jonathan van den Berg et al.

(submitted to Nuclear Fusion)

Plasma flux measurements

Plasma volume

Incoherent Thomson Scattering (TS): $n_e,\ T_e$

Coherent Thomson Scattering (CTS): $v_i,\ T_i$

TS + CTS: $\Gamma,\ p^{tot},\ q_{||}$

Target surface

Pyrometer + IR camera: T_{surf}

In-target thermocouple: q

In-target Langmuir probe for $I_{sat} = e\Gamma_t$

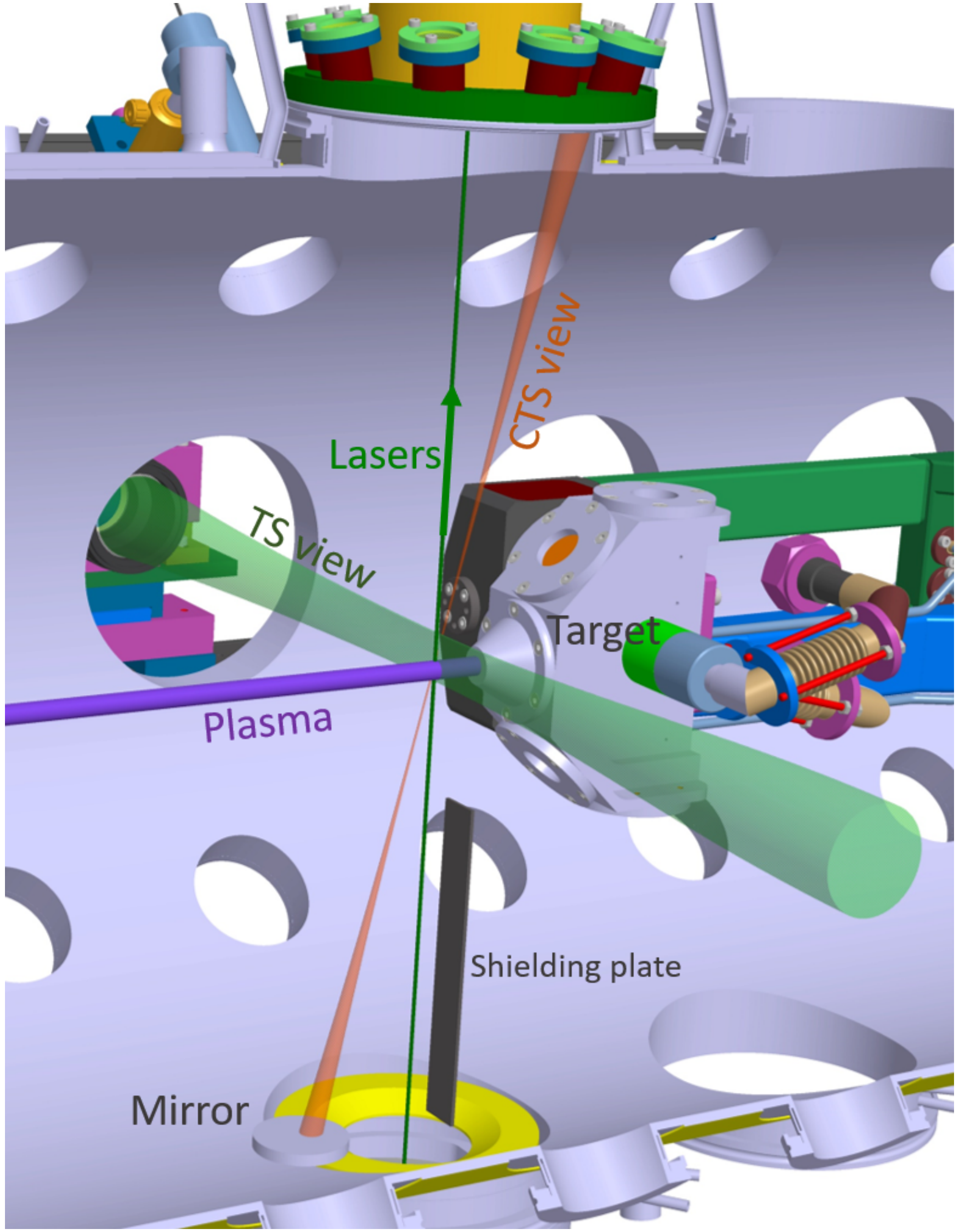

Parallel plasma velocities

At $d_{target-laser} = 25\ mm$

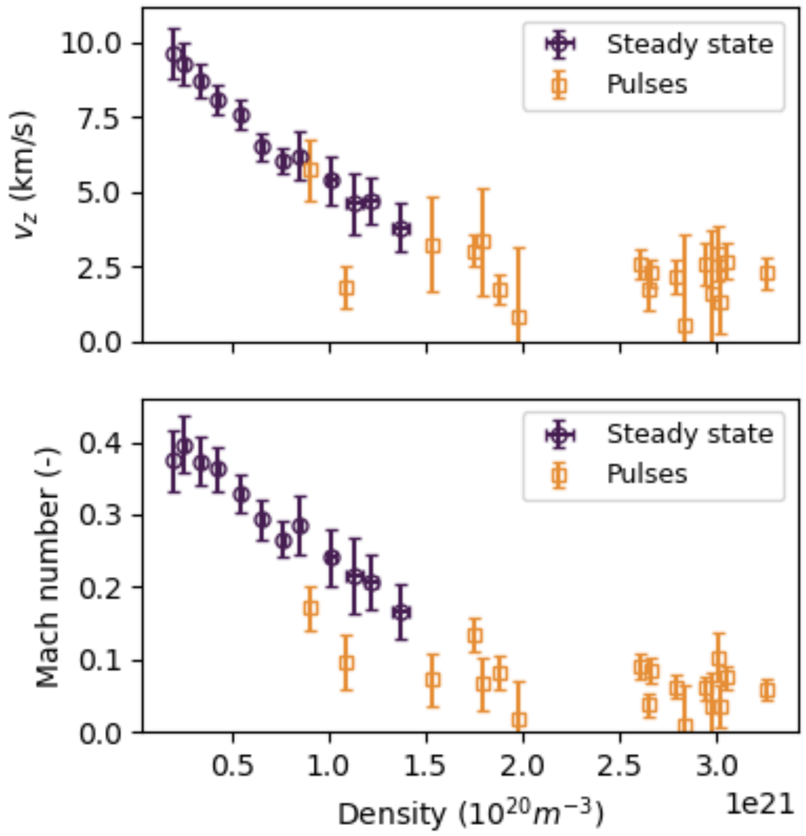

- Velocity decreases with density
- Same for the Mach number $M = \dfrac{v}{c_s}$
- Almost complete stagnation during pulses
- Momentum conservation under isothermal conditions:
  $$\mathrm{M_u} = \frac{n_{se}}{n_u} = \frac{1}{M_{se}^2 + 1} = \frac{1}{2}$$
- Lower M implies higher momentum losses in near wall region

TS and CTS results

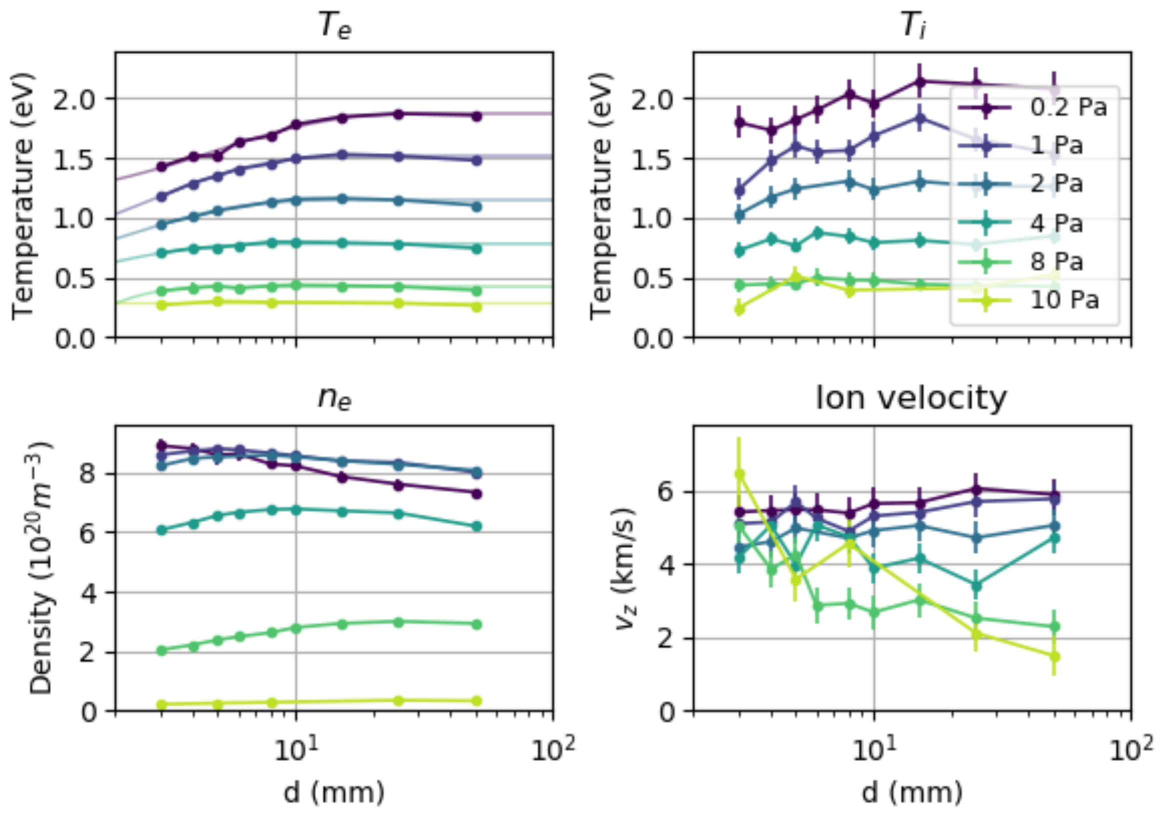

At low n_e:

- Constant T
- Pre-sheath accellerarion toward M=1 (Bohm)

At high n_e:

- Cooling towards wall
- No acceleration / stagnation, M well below 0.5

At high n_e ➔ losses to neutrals

(Energy and momentum losses in near wall region confirmed by comparison with target fluxes)

Losses to neutrals: 0D model

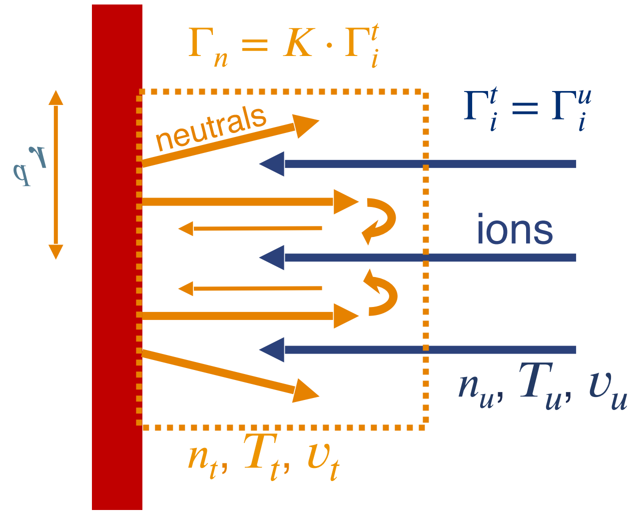

Simplified 0D model was derived to predict losses in p-n interaction region

- Recombining neutrals diffuse radially out
- Recombination, ionization and CX

➔ Loss factors depend on density:
Substantial losses in dense conditions

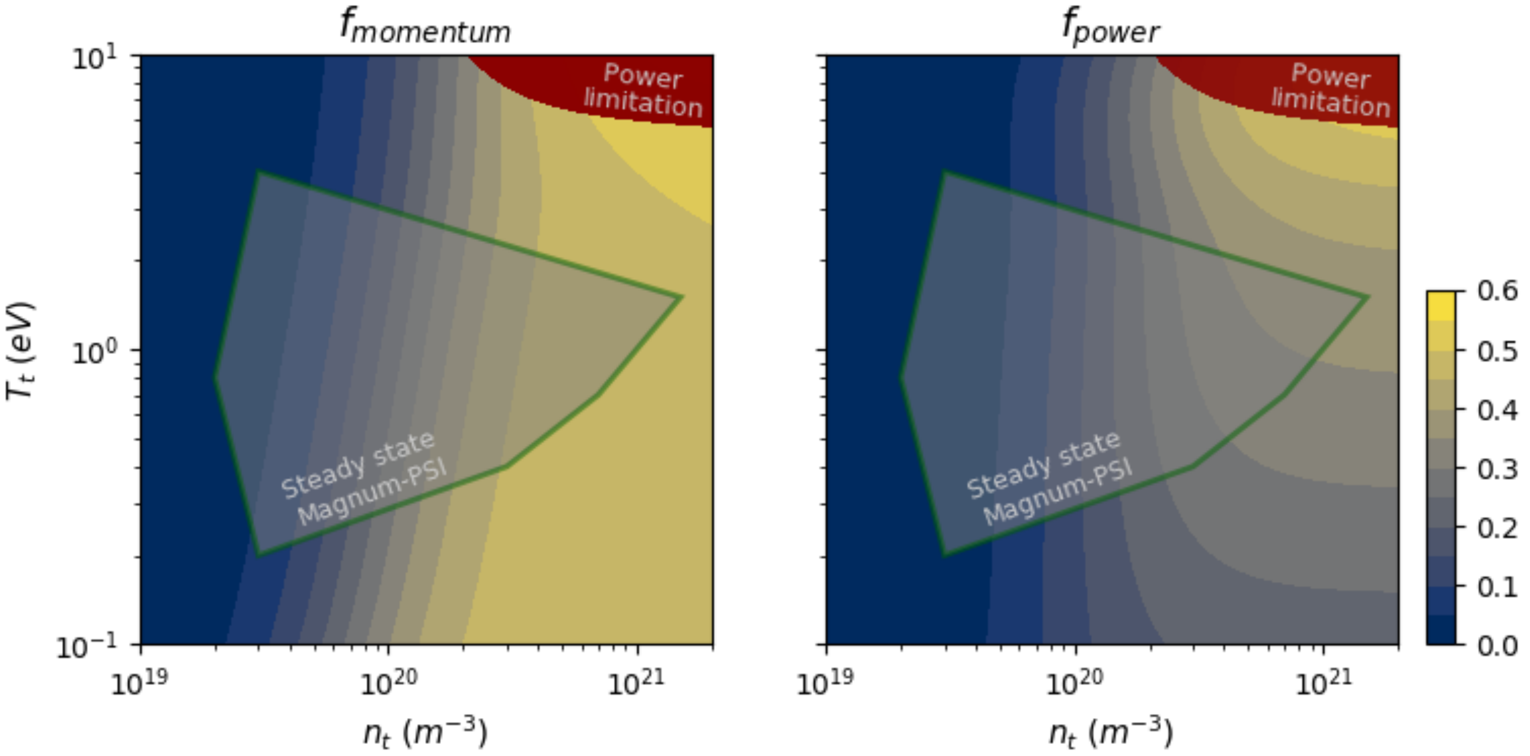

Implications of near wall p-n coupling

- Pre-sheath acceleration not experimentally observed in high densities:
  ➔Must occur in < 3mm
- Mach number still far below 0.5 at 3mm
  ➔ momentum loss region is very narrow
  ➔ strong gradients

Modelling:

- Near wall resolution of SOL models should be high enough:
  $d_{grid} < \lambda_{neutral\ mfp}$
- If grid size too course the sheath boundary condition (Bohm) might fail: M < 1

Section D

Plans for VUV-LIF on Magnum-PSI: $H_2(r,\nu)$

Motivation

- The ro-vibrational distribution plays a major role:
  MAR rate can vary multiple orders of magnitude

- Direct measurement difficult, but $H_2(r,\nu)$ distribution previously successfully measured in both linear plasmas and tokamaks (no current set-ups)

- ➔ Build new diagnostic on Magnum-PSI (divertor relevant plasmas) based on proven methods: VUV-LIF and CARS

- Grant application running at Dutch Scientific Organization (NWO)

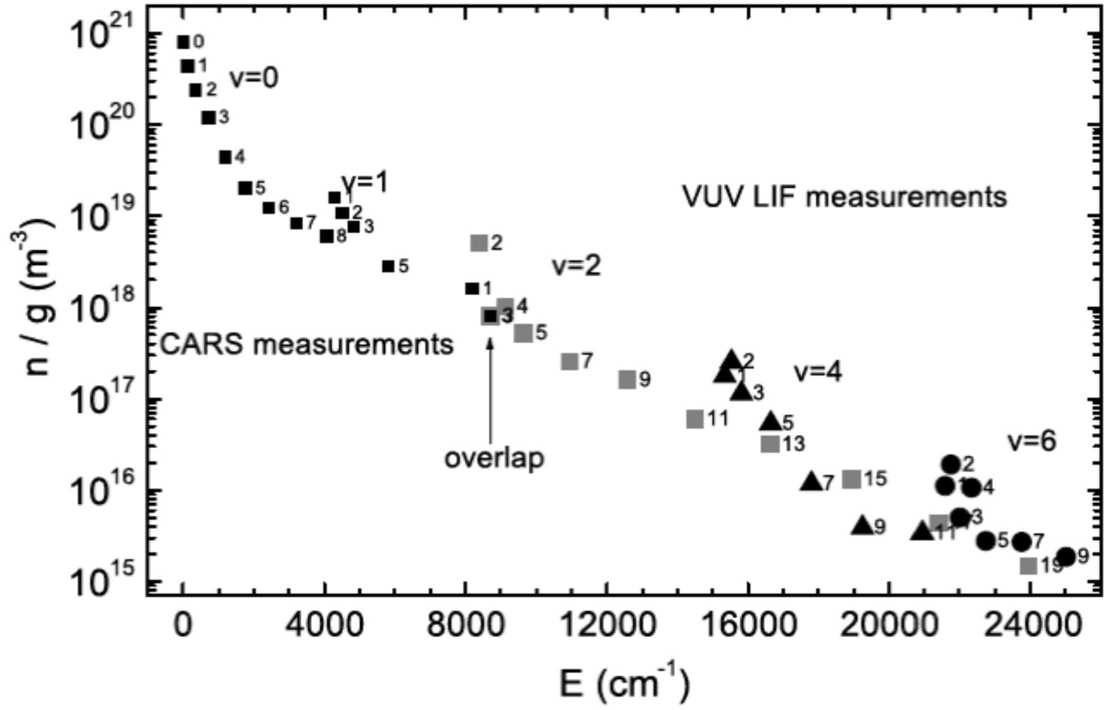

From Vankan et al.

Active spectroscopy: 3 methods

- Deploy active spectroscopy for complete exploration of ro-vibrational distribution of H_2 ground state:

- **VUV-LIF** based on Stimulated anti-Stokes Raman scattering (population ν >2,J)

- Coherent anti-Stokes Raman spectroscopy (**CARS**): (population $\nu \leq 2$,J)

- Two photon Absorption Laser Induced Fluorescence (**TALIF**) (density H atoms in ground state)

VUV-LIF principle

- Excite ground state ro-vib level to electronically excited state
- Measure fluorescence signal
- Scanning the laser wavelength excites different ro-vib states
- 110 to 165 nm for ν=0 to ν=14

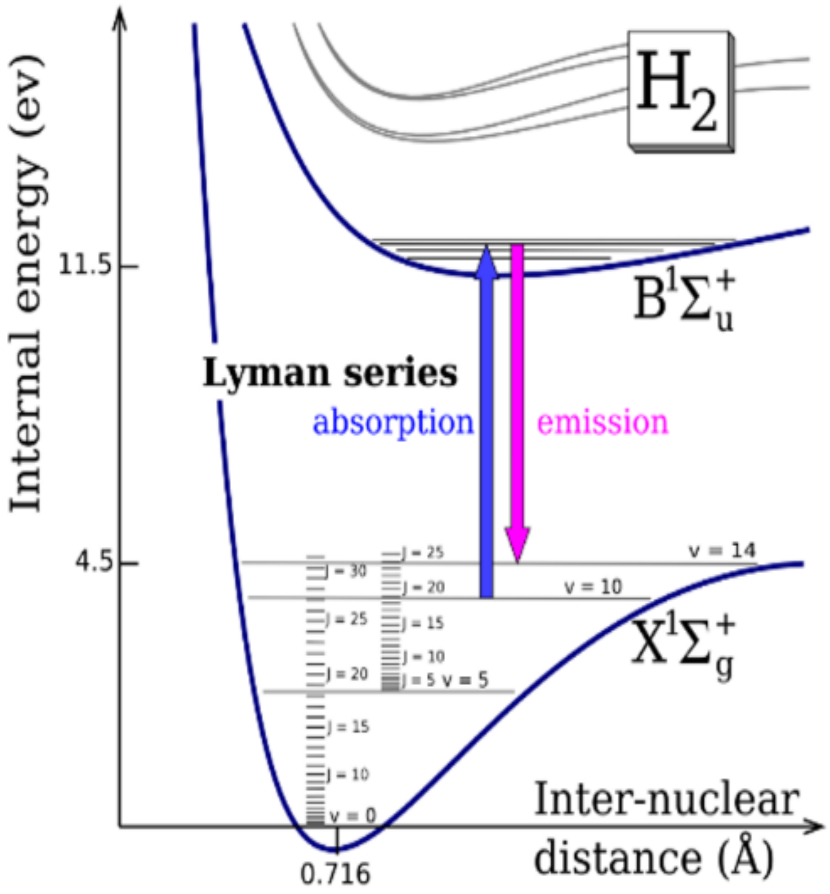

VUV LIF spectroscopy of H_2 ground state

Planned VUV-LIF setup

- Laser in VUV range (down to ~ Ly α)

➔ Raman cell (SARS)

- In vacuum
- VUV monochromators
- Vacuum window transmission (>120 nm) prevents measuring lower vibrational states (ν>2)

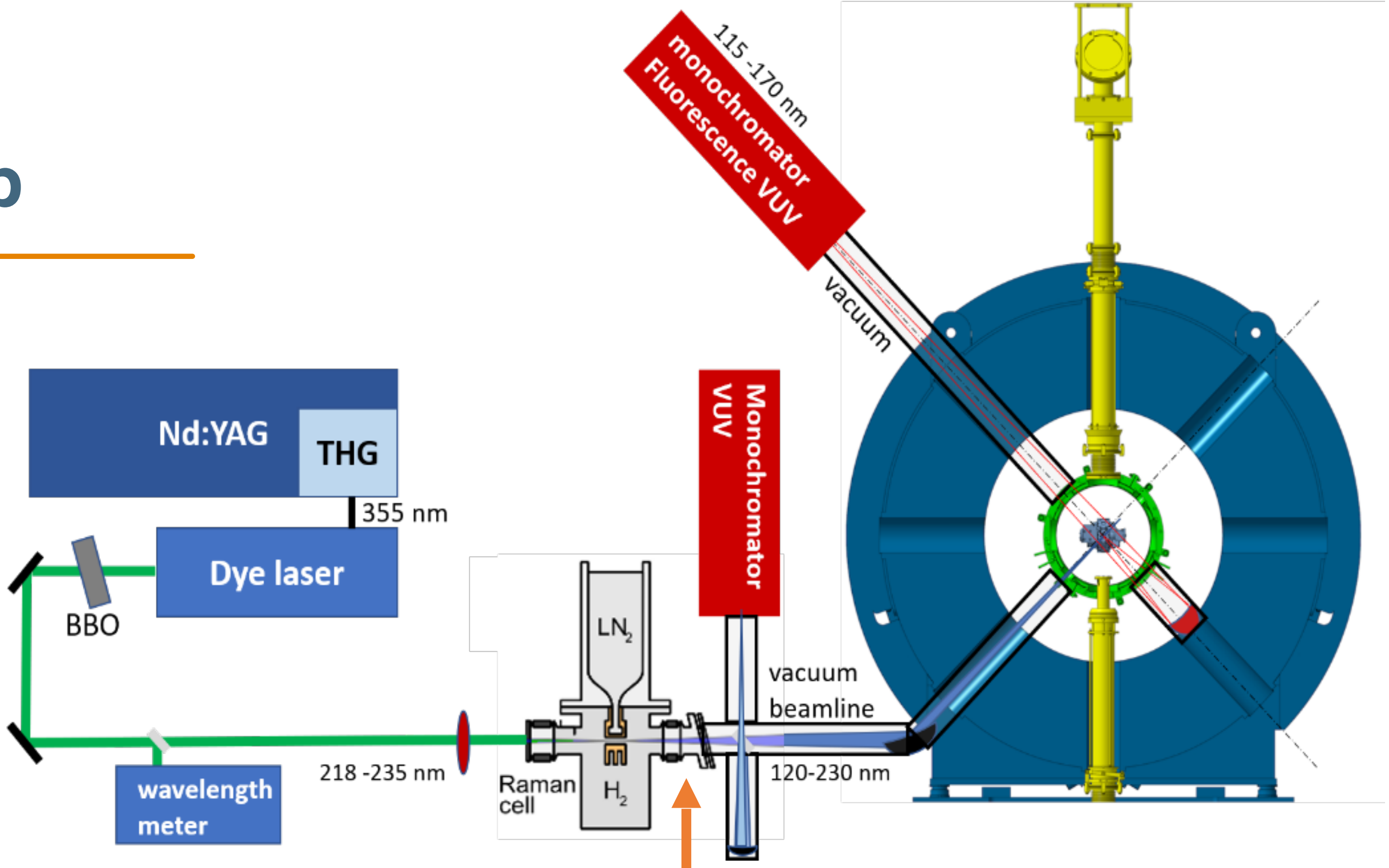

Complementary techniques: CARS

Lower vibrational states (ν<=2) can be measured with CARS

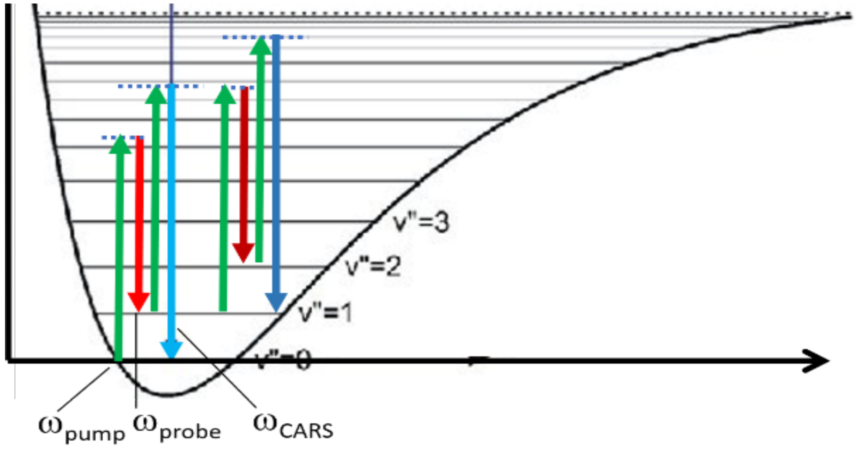

- Same lasers as VUV-LIF
- No vacuum needed

- CARS:
  4-wave mixing process
  660-700 nm probe beam
  532 nm pump beam

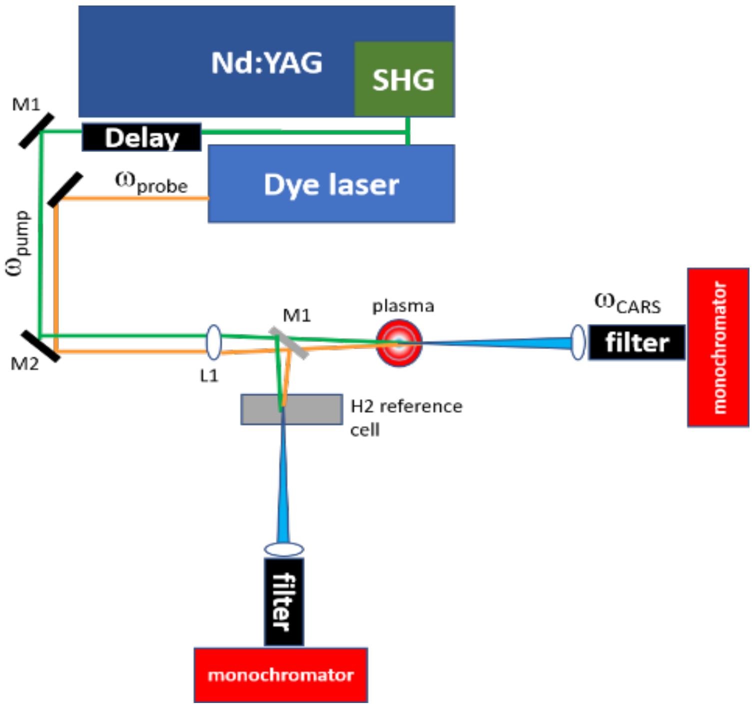

Complementary techniques: TALIF

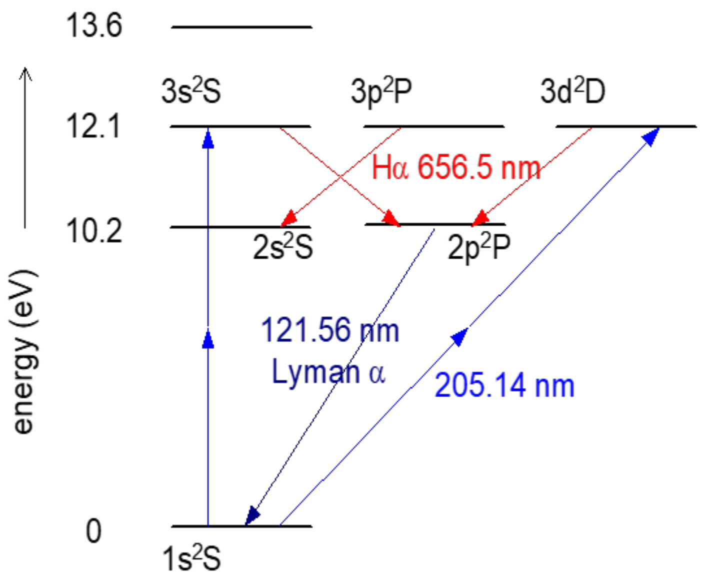

TALIF:

- Density of atomic H density
  Also applicable to N

- Excitation: 205.14 nm
  (for Ly β absorption with 2 photons)
- Fluorescence: Hα

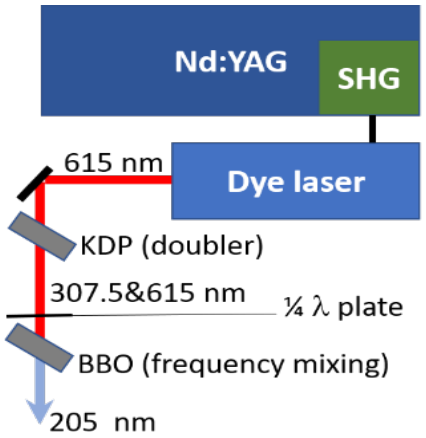

Together with existing diagnostics, these active spectroscopy methods would provide a uniquely complete picture of the (molecular) processes in divertor plasmas

Magnum-PSI welcomes your experiments!

- Well diagnosed
- Accessible
- Simple geometry
- Steady state plasma

Contact: i.g.j.classen@differ.nl

DIFFER